(12) INTERNATIONAL APPLICATION PUBLISHED UNDER THE PATENT COOPERATION TREATY (PCT)

(19) World Intellectual Property Organization
International Bureau

(43) International Publication Date
20 July 2017 (20.07.2017)

WIPO | PCT

(10) International Publication Number
WO 2017/123186 A1

(51) International Patent Classification:
C22C 14/00 (2006.01) *C22F 1/18* (2006.01)

(21) International Application Number:
PCT/US2016/012786

(22) International Filing Date:
11 January 2016 (11.01.2016)

(25) Filing Language: English

(26) Publication Language: English

(71) Applicants: **GENERAL ELECTRIC COMPANY** [US/US]; 1 River Road, Schenectady, NY 12345 (US). **NATIONAL INSTITUTE FOR MATERIALS SCIENCE**; 1-2-1 Sengen, Tsukuba-city Ibaraki, 305-0047 (JP).

(72) Inventors: **MARTE, Judson, Sloan**; One Research Circle, Bldg K1-MB 131, Niskayuna, NY 12309 (US). **GIGLIOTTI, JR., Michael, Francis, Xavier**; 1 Research Circle, K1-MB177, Niskayuna, NY 12309 (US). **SUBRAMANIAN, Pazhayannur, Ramanathan**; One Research Circle, K1-MB201, Niskayuna, NY 12309 (US). **TETSUI, Toshimitsu**; One Research Circle, Niskayuna, NY 12309 (JP). **DHEERADHADA, Voramon, Supatarawanich**; 1 Research Circle, MB-223, Niskayuna, NY 12309 (US).

(74) Agents: **DICONZA, Paul, J.** et al.; General Electric Company, Global Patent Operation, 901 Main Avenue, 3rd floor, Norwalk, CT 06851 (US).

(81) Designated States *(unless otherwise indicated, for every kind of national protection available)*: AE, AG, AL, AM, AO, AT, AU, AZ, BA, BB, BG, BH, BN, BR, BW, BY, BZ, CA, CH, CL, CN, CO, CR, CU, CZ, DE, DK, DM, DO, DZ, EC, EE, EG, ES, FI, GB, GD, GE, GH, GM, GT, HN, HR, HU, ID, IL, IN, IR, IS, JP, KE, KG, KN, KP, KR, KZ, LA, LC, LK, LR, LS, LU, LY, MA, MD, ME, MG, MK, MN, MW, MX, MY, MZ, NA, NG, NI, NO, NZ, OM, PA, PE, PG, PH, PL, PT, QA, RO, RS, RU, RW, SA, SC, SD, SE, SG, SK, SL, SM, ST, SV, SY, TH, TJ, TM, TN, TR, TT, TZ, UA, UG, US, UZ, VC, VN, ZA, ZM, ZW.

(84) Designated States *(unless otherwise indicated, for every kind of regional protection available)*: ARIPO (BW, GH, GM, KE, LR, LS, MW, MZ, NA, RW, SD, SL, ST, SZ, TZ, UG, ZM, ZW), Eurasian (AM, AZ, BY, KG, KZ, RU, TJ, TM), European (AL, AT, BE, BG, CH, CY, CZ, DE, DK, EE, ES, FI, FR, GB, GR, HR, HU, IE, IS, IT, LT, LU, LV, MC, MK, MT, NL, NO, PL, PT, RO, RS, SE, SI, SK, SM, TR), OAPI (BF, BJ, CF, CG, CI, CM, GA, GN, GQ, GW, KM, ML, MR, NE, SN, TD, TG).

Published:

— *with international search report (Art. 21(3))*

(54) Title: TIAL-BASED ALLOYS HAVING IMPROVED CREEP STRENGTH BY STRENGTHENING OF GAMMA PHASE

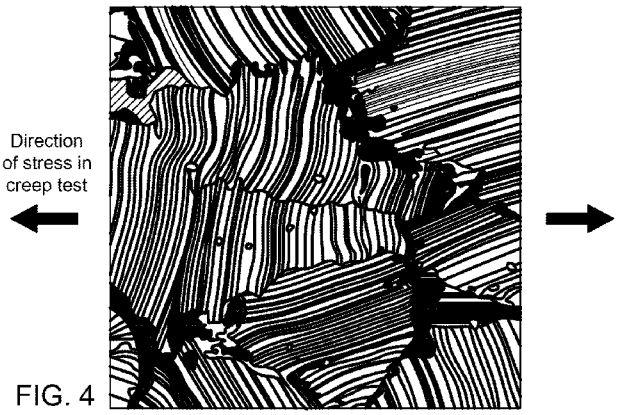

FIG. 4

(57) Abstract: A TiAl-based alloy having an excellent high-temperature creep strength are provided. According to one embodiment, the TiAl-based alloy comprises, in atomic percent, about 42.5 % to about 45.5 % aluminum (Al), about 8.0 % to about 15.0 % niobium (Nb), about 0.3 % to about 0.8 % carbon (C), about 0.3 % to about 0.9 % silicon (Si), balance titanium (Ti) and incidental impurities. A method of producing an article comprising the step of casting the TiAl-based alloy, and an article made from the TiAl-based alloy are also provided.

WO 2017/123186 A1

TiAl-BASED ALLOYS HAVING IMPROVED CREEP STRENGTH BY STRENGTHENING OF GAMMA PHASE

TECHNICAL FIELD

[0001] The subject matter disclosed herein generally relates to a TiAl-based alloy, in particular, to a TiAl-based alloy suitable for use in high-temperature applications, for example, turbomachinery components such as gas turbine blades for aviation and power-generation. Specifically, the subject matter disclosed herein relates to a TiAl-based alloy having improved creep strength.

BACKGROUND

[0002] TiAl-based alloys, a class of intermetallic alloys based on Ti and Al, have attracted much attention over the last several decades as novel light-weight high-temperature metallic materials, and have been the subject of intense research and development. As a result of such efforts, those alloys have been reduced to practice in recent years as components such as turbine last-stage blades of jet engines and/or turbine wheels in automotive turbochargers. As improvements in efficiency and fuel economy, as well as in CO_2 reduction, are continuously sought in a wide variety of fields such as energy and transportation, there is a desire to expand the use of TiAl-based alloys which potentially contribute to such needs.

[0003] In order to increase the use of TiAl-based alloys, it is necessary to develop a material that can be used in components operated at higher temperature as compared with those for which conventional TiAl-based alloys have been used. To achieve this, a significant improvement of creep strength is required.

[0004] Improvement of creep strength of a TiAl-based alloy is typically achieved by adjustment of its composition and conditions for heat treatment to prepare a material substantially consisting of lamellar microstructures comprising layers of alpha2 ($\alpha 2$) phase (Ti3Al phase) and gamma (γ) phase (TiAl phase). The lamellar structure is formed during cooling process from elevated temperatures, and the phase transition

process may be represented as follows:

$$\alpha \rightarrow \alpha + \gamma \rightarrow \alpha 2 + \gamma \qquad (1)$$

[0005] As a TiAl-based alloy typically forms single phase at a high temperature around 1330°C or above depending on its composition, the material becomes single phase under a high temperature state such as high temperature heat treatment or immediately after casting. In the course of cooling from such a high temperature state, gamma phase precipitates in the form of platelets (lamellae) within the alpha phase matrix, resulting in the formation of a lamellar structure comprising layers of alpha and gamma. This alpha phase is eventually transformed into alpha2 phase. Therefore, grains of alpha phase present at high temperatures turn into grains of the lamellar microstructure (i.e., lamellar colonies) finally obtained. The problem acknowledged herein is grain boundaries between alpha grains, i.e., interfaces between lamellar colonies in the final state.

[0006] Since an interface such as grain boundary generally provides a preferential site for precipitation, gamma phase precipitates preferentially at grain boundaries between alpha grains during cooling. In other words, even when a fully lamellar structure is formed in the final structure, the interface between the lamellar colonies is occupied by gamma phase extending in a thin planar form.

[0007] Alpha2 phase has a crystal structure of $D0_{19}$, while gamma phase has a crystal structure of $L1_0$, and hence the former structure is more complex. In consequence, alpha2 phase has greater high-temperature strength than gamma phase, although the former is more brittle.

[0008] Previous academic studies on creep mechanism of TiAl-based alloys have focused on evaluation of effects of various factors in the lamellar structure, including phase spacing and/or volume fraction of each phase in the lamellar structure, and required potential effects of boundary gamma phase with smaller high temperature strength to be excluded. Thus, experiments were conducted using a model specimen called PST (polysynthetic twin) crystal obtained by directional solidification as shown in FIG. 1 (cited from Yamaguchi, M., et. al., Mat. Sci. Eng. A213 (1996) 25-31; Fig. 2

at page 3). See also Lee, H.N. et. al., Intermetallics 10 (2002) 841-850; Asai, T., et. al.; Mat. Sci. Eng. A329-331 (2002) 828-834; and Maruyama, K. et. al., Intermetallics 13 (2005) 1116-1121. Since model material as shown in FIG. 1 has lamellar colonies aligned along the longitudinal direction of the specimen, gamma phase present at the interface between lamellar colonies also extends longitudinally.

[0009] FIG. 2 shows a relationship between the direction of stress loaded on this type of specimen during the creep test and thin plate-like gamma phase present at the interface between lamellar colonies. During the creep test, this gamma phase is subjected to tensile stress in a direction perpendicular to the plate thickness, but is hardly deformable in that direction because it is surrounded by lamellar structures of higher strength. Therefore, PST crystals as shown in FIG. 1 have been widely used as a test specimen in academic studies because creep mechanism can be analyzed while avoiding effects of relatively weak gamma phase.

[0010] However, currently it is not feasible to produce TiAl-based alloys for use in industrial applications by a directional solidification process. Therefore, such TiAl-based alloys made in the form of fully lamellar structure inevitably contain lamellar colonies that are randomly oriented in every direction. Consequently, random orientation is also observed for thin plate-like gamma phase present at boundaries between such lamellar colonies. FIG. 3 schematically illustrates a relationship between the direction of creep stress loaded during the high temperature use of a TiAl-based alloy having a fully lamellar structure manufactured by an industrial process and thin plate-like gamma phase at boundaries between lamellar colonies. As can be seen from FIG. 3, there always exists a boundary gamma phase that is subjected to tensile stress in a direction parallel to the plate thickness. In such a case, constraint force by surrounding lamellar structures is small and the creep stress is directly loaded to the gamma phase, leading to creep deformation of gamma phase and ultimately a failure.

[0011] Several attempts have been made to improve creep strength of TiAl-based alloys. See JP 2008-184665A; JP 2000-199025A; JP H10-130756A; JP H09-176764A; and JP H07-252562A. These publications disclose addition of elements such as Nb, C, and/or Si, to improve creep strength of TiAl alloy, whereby achieving

some improvement of creep strength over conventional TiAl-based alloys. However, the level of improvement is still insufficient for TiAl-based alloys intended for use in higher temperature applications.

[0012] Accordingly, it would be desirable to provide a TiAl-based alloy with significantly improved creep strength by an industrially-feasible process.

SUMMARY OF INVENTION

[0013] According to one aspect, the present invention provides a TiAl-based alloy comprising:

about 42.5 to about 45.5 atomic percent aluminum (Al);

about 8.0 to about 15.0 atomic percent niobium (Nb);

about 0.3 to about 0.8 atomic percent carbon (C); and

about 0.3 to about 0.9 atomic percent silicon (Si). The balance is titanium (Ti) and incidental impurities.

[0014] According to another aspect, the present disclosure provides a method for producing an article comprising a step of casting a TiAl-based alloy having a composition as described above, as well as an article made from the TiAl-based alloy.

[0015] These and other advantages and features will become more apparent from the following description taken in conjunction with the drawings.

BRIEF DESCRIPTION OF THE DRAWINGS

[0016] The subject matter, which is regarded as the invention, is particularly pointed out and distinctly claimed in the claims at the conclusion of the specification. The foregoing and other features, and advantages of the invention are apparent from the following detailed description taken in conjunction with the accompanying drawings in which

[0017] FIG. 1 is a perspective view of a model material obtained by directional

solidification conventionally used in academic studies on creep mechanism of TiAl-based alloys (cited from Yamaguchi, M., et. al., Mat. Sci. Eng. A213 (1996) 25-31);

[0018] FIG. 2 is a schematic view showing a relationship between thin gamma phase at colony boundary of lamellar structure and the direction of stress loaded on a specimen as shown in FIG. 1 used for creep test;

[0019] FIG. 3 is a view showing a relationship between the direction of creep stress loaded during the high temperature use of a TiAl-based alloy having a fully lamellar structure manufactured by an industrial process and thin plate-like gamma phase present at boundaries between lamellar colonies;

[0020] FIG. 4 is a view showing an exemplary microstructure around the fracture position observed after the creep test of a TiAl-based alloy having a fully lamellar structure manufactured by an industrial process;

[0021] FIG. 5 is a view of an exemplary microstructure of a TiAl-based alloy having a duplex structure;

[0022] FIG. 6 is a view of a TiAl-based alloy ingot according to one embodiment;

[0023] FIG. 7 shows a microstructure of a TiAl-based alloy (backscattered electron image; the same shall apply to the subsequent figures) of a composition of alloy 1 as a comparative example;

[0024] FIG. 8 shows a microstructure of a TiAl-based alloy of a composition of alloy 2 as a comparative example;

[0025] FIG. 9 shows a microstructure of a TiAl-based alloy of a composition of alloy 3 according to the present disclosure;

[0026] FIG. 10 shows a microstructure of a TiAl-based alloy of a composition of alloy 4 according to the present disclosure;

[0027] FIG. 11 shows a microstructure of a TiAl-based alloy of a composition of alloy 5 according to the present disclosure;

[0028] FIG. 12 shows a microstructure of a TiAl-based alloy of a composition of alloy 6 according to the present disclosure;

[0029] FIG. 13 shows a microstructure of a TiAl-based alloy of a composition of alloy 7 as a comparative example;

[0030] FIG. 14 shows a microstructure of a TiAl-based alloy of a composition of alloy 8 as a comparative example;

[0031] FIG. 15 shows a microstructure of a TiAl-based alloy of a composition of alloy 9 according to the present disclosure;

[0032] FIG. 16 shows a microstructure of a TiAl-based alloy of a composition of alloy 10 according to the present disclosure;

[0033] FIG. 17 shows a microstructure of a TiAl-based alloy of a composition of alloy 11 as a comparative example;

[0034] FIG. 18 shows a microstructure of a TiAl-based alloy of a composition of alloy 12 according to the present disclosure;

[0035] FIG. 19 shows a microstructure of a TiAl-based alloy of a composition of alloy 13 according to the present disclosure;

[0036] FIG. 20 shows a microstructure of a TiAl-based alloy of a composition of alloy 14 according to the present disclosure;

[0037] FIG. 21 shows a microstructure of a TiAl-based alloy of a composition of alloy 15 as a comparative example;

[0038] FIG. 22 shows a microstructure of a TiAl-based alloy of a composition of alloy 16 according to the present disclosure;

[0039] FIG. 23 shows a microstructure of a TiAl-based alloy of a composition of alloy 17 according to the present disclosure;

[0040] FIG. 24 shows a microstructure of a TiAl-based alloy of a composition of alloy

18 according to the present disclosure;

[0041] FIG. 25 shows a microstructure of a TiAl-based alloy of a composition of alloy 19 as a comparative example;

[0042] FIG. 26 shows a microstructure of a TiAl-based alloy of a composition of alloy 20 according to the present disclosure;

[0043] FIG. 27 shows a microstructure of a TiAl-based alloy of a composition of alloy 21 according to the present disclosure; and

[0044] FIG. 28 shows a microstructure of a TiAl-based alloy of a composition of alloy 22 according to the present disclosure.

DETAILED DESCRIPTION

[0045] In an investigation leading to the present invention, the inventors discovered that, in order to improve the creep strength of industrial TiAl-based alloys, it is necessary to enhance the strength of gamma phase itself which is relatively low.

[0046] For example, in a TiAl-based alloy having a fully lamellar structure manufactured by an industrial process, rather than a model material as illustrated in FIG. 1, rupture is usually observed at boundary gamma phase between lamellar colonies, as described hereinbefore. One example is shown in FIG. 4. This figure illustrates a microstructure around the fracture position observed after the creep test on this type of TiAl-based alloy. As can be seen, cracks are observed only at boundary gamma phase oriented perpendicular to the direction of stress loaded during the creep test. No cracks are found within the lamellar structure. This indicates that, in order to improve the creep strength of industrial TiAl-based alloys, it is necessary to strengthen not only the interior lamellar structure, but also the thin plate-like gamma phase at lamellar colony boundary.

[0047] Besides those of a fully lamellar structure, other types of TiAl-based alloy materials are sometimes used when enhanced room temperature ductility is required, such as one comprising a microstructure having an increased proportion of equiaxed

grains of gamma phase, present separately from the lamellar structure. One example includes structure generally referred to as a duplex structure. FIG. 5 shows an exemplary microstructure of the duplex structure. The duplex structure includes both equiaxed gamma grains and lamellar structures, and exhibits greater room temperature ductility as compared with the fully lamellar structure, due to finer microstructure as a whole, and also because of increased proportion of gamma phase which is more ductile than alpha2 phase.

[0048] For these structures having equiaxed gamma grains such as duplex structure, it is also necessary to strengthen equiaxed gamma grains, the high-temperature strength of which is lower than the lamellar structure, in order to improve the creep strength.

[0049] As described above, in order to improve the creep strength of industrial TiAl-based alloys, it is necessary to enhance the strength of gamma phase itself which is relatively low, regardless of their microstructural morphology such as fully lamellar structure or duplex structure.

[0050] As mentioned above, the crystal structure of gamma phase is a $L1_0$ structure based on fcc. Since it is intermetallic phase, Ti and Al atoms are located at specific lattice positions, rather than random arrangement of atoms in a crystal. Thus, unlike fcc, the ratio of lattice constants of c-axis and a-axis ("c/a") is not equal to 1, and is characterized by somewhat larger c-axis. For example, gamma phase of Ti50:Al50 atomic percent (%) has a slightly distorted lattice with a c/a ratio of about 1.02.

[0051] Without being bound to any particular theory, the present inventors have envisaged that if the c/a ratio of gamma phase is further increased the lattice can be further distorted, which affects to hinder movement of dislocation during creep deformation, making the gamma phase more resistant against creep deformation. It is also believed that this approach can be effectively utilized to improve the creep strength of the material through the improvement of strength of boundary gamma phase, because the gamma phase at the lamellar colony boundary is a key factor that dominates the material creep strength even for those materials solely comprising a fully lamellar structure which itself is advantageous for improvement of the creep

strength, as described above.

[0052] As mentioned above, prior publications disclosed addition of elements such as Nb, C, and Si to improve the creep strength of TiAl-based alloys. However, the level of creep strength was not sufficient for high temperature applications. The present inventors proposed that, in order to further improve creep strength, it is necessary to strengthen the gamma phase. In this aspect, the present inventors discovered that Nb at levels higher than the level included in the prior art helped to further strengthen the gamma phase, thus improving creep strength of the alloys. However, interactions between Nb and Al can be significant. Moreover, an unduly high level of Nb may stabilize the beta phase, which is soft and can be detrimental to high temperature creep strength. Thus, in designing the alloys, one cannot merely increase Nb level. Rather, a careful design of alloy compositions has to be done as shown by the present inventors.

[0053] With respect to the Al content, most of Nb added at a conventional level substitutes for Ti and little substitution occurs for Al (i.e., addition of Nb causes only a little change in the Al equivalent). Thus, a suitable Al content for an Nb-containing TiAl-based alloy was conventionally considered to be similar to that of ordinary TiAl alloys. For example, the Al content taught by the prior art was: 31-34 wt.% (JP 2008-184665A); 44.5-48.5 at.% (JP 2000-199025A); 44-48 at.% (JP H10-130756A); 29-30.5 wt.% (JP H09-176764A); and 32-36 wt.% (JP H07-252562A). If the Nb content is substantially higher than the conventional level, however, a substantial change occurs in the Al equivalent because the amount of substitution of Al by Nb, although still small in terms of relative proportion, becomes substantial in terms of absolute amount. The present inventors have investigated for the first time an Al range in this aspect.

[0054] Carbon strengthens TiAl-based alloys as an interstitial solid solution element, and JP 2008-184665A teaches the addition of C at a level up to 0.12 wt.%. Although the addition of C may cause an unfavorable reduction in the creep strength or embrittlement due to formation of large carbide, Ti_2AlC, small addition of carbon may help to strengthen the alloys. The present inventors investigated effects of carbon in

this respect.

[0055] Silicon (Si) is an additive for precipitation strengthening of TiAl-based alloys, and is typically used in a range of 0.1-0.7 wt.% (JP 2008-184665A); 0.1-0.4 at.% (JP 2000-199025A); 0.2-0.5 at.% (JP H10-130756A); 0.1-0.2 wt.% (JP H09-176764A); and 0.1-2 wt.% (JP H07-252562A). Although the volume fraction of precipitates may be increased depending on the amount of Si to be added, excess addition may cause coarsening of the precipitates, leading to an unfavorable reduction in the creep strength or embrittlement.

[0056] After extensive investigations on each element composition in view of the above, the present inventors have successfully obtained a TiAl-based alloy with substantially improved creep strength as compared with conventional alloys. According to one embodiment, the TiAl-based alloy has a composition:

Al: about 42.5-45.5 at.%;

Nb: about 8.0-15.0 at.%;

C: about 0.3-0.8 at.%;

Si: about 0.3-0.9 at.%; and

Ti: the balance, and incidental impurities.

[0057] In one embodiment the TiAl-based alloy may comprise Nb in a range of from about 9.0 atomic percent to about 11.0 at.%. In another embodiment, the TiAl-based alloy may comprise Nb in a range of about 9.3 at.% to about 11.0 at.%.

[0058] The TiAl-based alloy may further comprise at least one element selected from the group consisting of W, Zr, and Ta, in a total amount up to about 3.0 at.%. One or more of these elements may be added to further improve the creep strength by enhanced strengthening of gamma phase.

[0059] According to another aspect, the present disclosure provides a method for producing an article comprising a step of casting a TiAl-based alloy having a

composition as described above, as well as an article made from the TiAl-based alloy

[0060] For example, a variety of articles, including turbine blades, may be prepared by melting and casting a TiAl-based alloy having a composition as described above.

[0061] In one embodiment, the method of producing an article may comprise a post-processing step after casting a TiAl-based alloy. Such a post-processing may include heat treatment and/or forging.

[0062] In one embodiment, the post-casting heat treatment of the TiAl-based alloy may comprise holding the as-cast article at a high temperature.

[0063] The high-temperature holding may be conducted at a temperature for a period of time sufficient to make the entire material into a single phase region. In one embodiment, the cast article may be maintained at a temperature of about 1280°C or above, and more particularly, 1300°C or above, such as 1310-1390°C, for at least one hour, such as about 1-10 hours.

[0064] A material having a single alpha phase thus obtained may be subjected to controlled cooling regime. In one embodiment, the cooling condition may be suitably adjusted depending on a particular alloy composition so as to cause a desired level of gamma precipitation through transformation such as $\alpha \rightarrow \alpha + \gamma \rightarrow \alpha 2 + \gamma$, to obtain a desired microstructure (for example, a fully lamellar structure, a duplex structure, or the like). In one embodiment, alloy microstructure may comprise up to about 20 at.% of primary gamma TiAl. The material may be allowed to cool in a same furnace used for the high-temperature holding, without removing it from the furnace, or may be removed from the furnace and cooled under the controlled cooling regime. Alternatively, the material may be subjected to quenching.

[0065] In another embodiment, the post processing step may comprise forging. The alloy may be preheated to a high temperature, for example, to such a temperature range that the alloy comprises 5% or more beta phase. In one embodiment, the preheat temperature is on the order of 1300-1350°C.

[0066] In one embodiment, the forging step may be carried out by placing a TiAl-

based alloy onto forging dies. In one embodiment, the dies may be lubricated. A glass sheet may be used as a lubricant, in which case the glass also acts as a thermal barrier during the initial portion of the forging operation. Additionally or alternatively, the dies may be heated to minimize transfer of heat from the alloy to the dies. In one embodiment, the dies may be heated to about 900°C for this purpose.

[0067] The forging operation may be carried out by applying load to a TiAl-based alloy while the alloy is hot at a low strain-rate. In one embodiment, forging may be carried out at a constant strain-rate of about 0.6 in/in/min (10^{-2} s^{-1}) to strain of 50%. Then, the alloy may be allowed to air cool.

[0068] The article may be used in a wide variety of applications including, for example, various components in turbomachinery, such as turbine blades, compressor blades, seals, and other components within industrial gas turbines for power generation; low pressure turbine blades, high pressure compressor blades, shrouds, and seals within aircraft engines for propulsion and auxiliary power generation; impellers, radial compressors, and turbine wheels within turbochargers for diesel and gasoline reciprocating engines; and any other application that can benefit from use of the high-temperature light-weight materials with improved creep strength.

[0069] More detailed discussion will be provided below about each of the elements and their contents of the TiAl-based alloy composition. It should be noted that any reference to percentage hereinafter is in atomic percentage (at.%), unless explicitly stated otherwise.

Aluminum (Al)

[0070] Aluminum is an essential element constituting a TiAl-based alloy, and it was long considered that an Al level for a traditional TiAl-based alloy is suitably around 46 at.%. The Al content affects the proportion of gamma phase to alpha2 phase in the lamellar structure. As it deceases the proportion of alpha2 phase increases, while the proportion of gamma phase increases as the Al content increases. The Al level also affects the c/a ratio of gamma phase, such that a higher Al content results in a greater c/a. While niobium (Nb) basically substitutes for Ti, a portion of Nb also

substitutes for Al. The addition of Nb appears to have similar effects to some increase in the Al level, and therefore the Al level should be reduced when a large amount of Nb is to be added.

[0071] As discussed above, the Al content has complicated effects on the structure of the TiAl-based alloy as well as the lattice of gamma phase. After extensive investigations, the present inventors identified a range of 42.5-45.5 at.% Al to be suitable for improvement of creep strength. It should be noted that the Al content at a level of 46 at.% provides a sufficient proportion of alpha2 phase in the lamellar structure for a conventional TiAl-based alloy. For the alloy disclosed herein, in contrast, a suitable Al content is somewhat lower than the conventional TiAl-based alloy, because the addition of a large amount of Nb appears to have similar effects to some increase in the Al level, as described hereinbefore.

[0072] With the Al content at a level of less than 42.5 at.%, the c/a ratio of gamma phase tends to become too small to achieve a sufficient level of creep strength by strengthening of gamma phase. With the Al content at a level of greater than 45.5 at.%, the creep strength can decrease in association with an undesirably increased proportion of gamma phase and correspondingly decreased proportion of alpha2 phase in the lamellar structure.

Niobium (Nb)

[0073] Niobium at a range of 8.0-15.0 at.% strengthens gamma phase through an increased c/a ratio of gamma phase, and can significantly improve the creep strength of a TiAl-based alloy regardless of its microstructural morphology. With the Nb content at a level of less than 8 at.%, a certain degree of enhancement in the creep strength may be observed as in the prior art, but is still insufficient to achieve a higher level of creep strength as described herein. Niobium content greater than 15 at.% is generally undesirable, as it tends to decrease the creep strength due to formation of beta (β) or other detrimental phases, some of which arise as a result of other alloying elements and heat treatment conditions. It should be noted that beta (β) phase is an intermetallic phase in B2 structure which is a derivative of bcc structure, and is

characterized by poor high-temperature strength. Niobium is a beta-stabilizing element for TiAl-based alloys. Excess Nb may cause formation of beta phase, even though such an effect is small for a unit amount of the additive.

[0074] Niobium is about ten times more expensive than the other elements in the alloy, and also increases the density of TiAl-based alloy. For these reasons, it may be advantageous to limit the amount of Nb. By taking all these effects, such as enhanced creep strength, and increased cost and specific gravity, associated with the Nb addition into consideration, the Nb content may be chosen in a range of 9.0-11.0 at.% in one embodiment, or in a range of 9.3-11.0 at.% in another embodiment.

Carbon (C)

[0075] Carbon is an interstitial solid solution element for strengthening gamma phase, thus leading to further strengthening of gamma phase in addition to strengthening by Nb. In general, the carbon content may be suitably in a range of 0.3-0.8 at.%. With the C content at a level of less than 0.3 at.%, a certain degree of enhancement in the creep strength may be observed, but is still insufficient to achieve a higher level of creep strength. Carbon content greater than 0.8 at.% may cause formation of detrimental carbides such as Ti_2AlC beyond the solid solubility limit, although depending on other alloying elements and heat treatment conditions, which may lead to undesirably decreased creep strength.

Silicon (Si)

[0076] In one embodiment, silicon is added for precipitation strengthening of the whole structure. Most of the Si addition precipitates as fine Ti_5Si_3 particles, which leads to enhanced creep strength. In general, the Si content may be suitably in a range of 0.3-0.9 at.%. With the Si content at a level of less than 0.3 at.%, a certain degree of enhancement in the creep strength may be observed as in the prior art, but is still insufficient to achieve a higher level of creep strength. The Si content at a level of greater than 0.9 at.% may cause coarsening or excess precipitation of Ti_5Si_3, although depending on other alloying elementsand heat treatment conditions, which may lead to undesirably decreased creep strength.

Optional elements: W, Zr, Ta, Cr

[0077] Tungsten (W), zirconium (Zr) and tantalum (Ta) are elements which can contribute to further enhancement of the creep strength through additional strengthening of gamma phase, and may optionally be added alone or in any combination. In general, one or more of these element may be added in a total amount up to 3.0 at.%. The creep strength may be undesirably decreased at a level of greater than 3.0 at.%, due to formation of beta or other detrimental phases, although depending on other alloying elements and heat treatment conditions.

[0078] Chromium (Cr) may be added in an amount up to 0.5 at.%. Excess Cr may cause formation of beta phase, leading to undesirably decreased creep strength.

[0079] The TiAl-based alloy as disclosed herein shows a creep strength that is substantially higher as compared with conventional TiAl-based alloys. Accordingly, the TiAl-based alloy as disclosed herein may be advantageously used for a variety of components in various machineries in energy or transportation fields, including those components for which conventional TiAl-based alloys could not be used: for example, turbine blades in a higher temperature section in power generation gas turbines and/or aviation jet engines, and turbine wheels in automotive turbochargers operated at higher temperatures, whereby further improvement of efficiency and fuel economy, and CO_2 reduction may be achieved.

EXAMPLES

[0080] The present invention will be further illustrated by way of the following examples with reference to the accompanying drawings.

Table 1 Summary of compositions of prototype ingots and results of their assessment

Alloy No.	Type*	Elements (at.%)									Heat Treatment Conditions	Creep Rupture Time (h)**
		Al	Nb	Si	C	Cr	W	Zr	Ta	Ti		
1	C	46.50	3.20	0.50	0.20					bal	1350°C×3h → FC → 1000°C×10h	36
2	C	43.65	10.50	0.75	0.65	0.60				bal	1345°C×3h → FC →	57

											1000°C×10h	
3	E	43.00	8.80	0.80	0.80					bal	1440°C×2h → 1285°C×5h → 8°C/min → 1000°C×8h	107
4	E	43.35	8.00	0.65	0.54					bal	1360°C×1h → 5°C/min → 1000°C×10h	128
5	E	44.25	11.5	0.75	0.575					bal	1370°C×3h → FC → 1000°C×10h	230
6	E	45.20	12.00	0.85	0.650					bal	1380°C×5h → FC	132
7	C	45.60	10.00	0.85	0.850					bal	1325°C×10h → AC → 1000°C×50h	52
8	C	43.70	7.40	0.85	0.60					bal	1310°C×4h → 10°C/min	103
9	E	43.65	9.0	0.75	0.65					bal	1370°C×1h → FC → 1000°C×7.5h	151
10	E	43.60	14.00	0.75	0.78					bal	1310°C×8h → 8°C/min → 1000°C×10h	141
11	C	44.00	16.00	0.55	0.75					bal	1325°C×5h → AC → 1000°C×10h	68
12	E	43.60	9.78	0.85	0.40					bal	1335°C×5h →→ FC → 1050°C×10h	94
13	E	44.25	10.00	0.75	0.50					bal	1370°C×5h → 10°C/min → 1000°C×7h	186
14	E	44.00	10.00	0.75	0.75					bal	1370°C×3h → FC → 1000°C×10h	158
15	C	43.60	12.50	0.85	0.84					bal	1280°C×10h → 12°C/min → 1000°C×7h	109
16	E	43.50	8.00	0.45	0.65					bal	1290°C×10h → FC → 1000°C×10h	89
17	E	43.60	9.84	0.55	0.60					bal	1335°C×20h → 2°C/min	130
18	E	43.6	10.20	0.85	0.60					bal	1365°C×5h → 10°C/min	137
19	C	43.30	10.20	0.95	0.60					bal	1365°C×5h → AC → 1000°C×10h	93
20	E	44.00	10.00	0.75	0.65		0.75			bal	1310°C×10h → FC → 1000°C×10h	225
21	E	44.00	10.00	0.75	0.65			1.5		bal	1390°C×5h → FC → 1000°C×10h	233

22	E	44.00	10.00	0.75	0.65				1.5	bal	1390°C×5h → FC → 1000°C×10h	192

*C: Comparative example; E: Example

**The rupture time (h) in creep rupture testing at 870°C × 225MPa

[0081] A number of ingots were made from TiAl-based alloys with different compositions as shown in Table 1 by a high-frequency induction melting process using an yttria crucible. Raw materials used for melting were: Ti sponge, Al pellets, and small Nb flakes with a thickness of about 0.5 mm, for Ti, Al and Nb, which were major elements in the alloys; and small particles for Si, Cr, W, Zr, and Ta. Carbon was added as TiC powder.

[0082] The melting atmosphere was argon gas, and after all the raw materials were completely melted, the molten material was held for further five minutes, and then poured into a mold made of cast iron, and solidified therein to form a cylindrical ingot. FIG. 6 shows an exemplary photograph showing appearance of a TiAl-based alloy ingot thus obtained. The dimensions of the ingot were 40 mm diameter (φ) × 100 mm, excluding a riser portion. The weight was about 800 gram in the as-cast state, from which the riser portion was cut off to give about 450 g.

[0083] In general, properties of a TiAl-based alloy depend not only on its particular composition, but also on its particular microstructural morphology. In the present examples, creep strengths were compared in microstructural morphologies that were as similar as possible to each other so that predominantly the effects of varying compositions could be evaluated. The target microstructural morphology was a fully lamellar structure which is advantageous for improvement of creep strength, and heat treatment conditions were adjusted for each alloy so as to make the resulting microstructures as similar as possible to each other. It should be noted that similar effects of alloy composition on creep strength are expected for other microstructural morphologies than the fully lamellar structure, although some decrease in the absolute values of creep strength may be observed.

[0084] For each alloy, ingots, from which a riser portion was cut off, were subjected

to the heat treatments as shown in Table 1. These conditions were chosen for each alloy based on the results of preliminary conducted heat-treatment tests. In the preliminary conducted heat-treatment tests, a number of test specimens were cut from the ingot of each alloy and were subjected to various heat treatment conditions, and optimal condition for achieving a lamellar structure was chosen based on microstructural examination of cross section of the heat-treated samples. The microstructure examination was conducted by scanning electron microscopy in the backscattered electron imaging mode.

[0085] The heat treatment conditions shown in Table 1 basically include steps of: holding at a high temperature; controlled cooling, and holding at a relatively lower temperature. Each of these steps was conducted for the following purpose:

[0086] (a) High-temperature holding: To solutionize the material.

[0087] (b) Controlled cooling: To cause transformations of $\alpha \rightarrow \alpha + \gamma \rightarrow \alpha 2 + \gamma$ during the cooling step so as to obtain a nearly fully lamellar microstructure by precipitation of gamma (γ) platelets. Because the amount of gamma precipitates depends on the cooling rate, as well as alloy composition (in particular, Al content), an appropriate cooling rate was chosen for each alloy. The term "FC" in Table 1 means furnace cooling, which was conducted by stopping the heating under a high temperature condition allowing the sample to cool in a furnace. The cooling rate in a furnace atmosphere of an electric furnace used in these experiments was 17°C/min until 1200°C. The term "AC" means air cooling, which was conducted by removing the sample from the furnace under a high temperature condition allowing it to cool under atmospheric condition. Although the exact cooling rate was not measured, the rate was supposed to be very high, such as 100°C/min or above.

[0088] (c) Holding at a relatively lower temperature: To stabilize the structure.

[0089] For these heat treatments, the holding time during the high-temperature heat treatment may be optimized to prevent coarsening of grains, resulting in a colony size that is not too coarse. In addition, the cooling rate may be optimized to obtain a microstructure having a suitable proportion of alpha2 and gamma phases in the

lamellar structure.

[0090] Microstructural examination and creep rupture test were conducted for each of the alloy ingots after the heat treatments. Creep rupture test was conducted at 870°C × 225MPa using a specimen with 4 mm diameter at parallel portion. The microstructure examination was conducted by scanning electron microscopy in the backscattered electron imaging mode. In the creep rupture test, creep strengths were compared between alloys based on creep rupture time.

[0091] The results of microstructural examination and creep rupture test conducted for Alloys 1-22 listed in Table 1 will be described below in more detail.

[0092] Alloy 1 is a comparative alloy, and its microstructure in a backscattered electron image (hereinafter the same) is shown in FIG. 7. Alloy 1 is based on a chemical composition disclosed in JP 2008-184665A. The microstructure was a fully lamellar structure advantageous for improvement of creep strength, as intended. The creep rupture time at 870°C × 225MPa was 36 hours, which is better than a TiAl-based alloy free of Si or C, but is still insufficient for applications where higher level of creep strength is required.

[0093] Alloy 2 is a comparative alloy, and its microstructure is shown in FIG. 8. Alloy 2 contained 0.6 at.% Cr beyond the compositional range according to the invention. Beta phase, which is seen in white, was present at interfaces between lamellar structures. Small white particles dispersed are Ti_5Si_3 precipitates formed due to the addition of Si.

[0094] As mentioned above, Nb is a weak beta-stabilizing element for TiAl-based alloys, but an excess amount of Nb tends to cause formation of beta phase. On the other hand, Cr is a very strong beta-stabilizing element. It appears that the addition of 0.6 at.% Cr caused formation of beta phase, even for such an alloy composition as disclosed herein in which beta formation is normally absent. The creep rupture time of Alloy 2 is shorter than the alloys according to the invention due to inferior high-temperature strength of beta phase.

[0095] Alloys 3-6 are alloys according to the invention, and their respective microstructures are shown in FIGS. 9-12. These alloys had different Al contents within the compositional range according to the invention. All of these alloys had a microstructure of lamellar structure, and showed a very long creep rupture time due to sufficient enhancement of gamma-phase strength.

[0096] Alloy 7 is a comparative alloy, and its microstructure is shown in FIG. 13. Alloy 7 represents a comparative alloy with a higher Al content outside the compositional range according to the invention. It had an excessive proportion of gamma phase (dark phase) with a reduced proportion of alpha2 phase (light phase) in the lamellar structure, resulting in a shorter creep rupture time than the alloys according to the invention.

[0097] Alloy 8 is a comparative alloy, and its microstructure is shown in FIG. 14. Alloy 8 represents a comparative alloy with a lower Nb content outside the compositional range according to the invention. Even though it had a microstructure of fully lamellar structure as intended, its creep rupture time was than the alloys according to the invention due to insufficient addition of Nb to strengthen gamma phase.

[0098] Alloys 9 and 10 are alloys according to the invention, and their respective microstructures are shown in FIGS. 15 & 16. Alloys 9 and 10 had different Nb contents within the compositional range according to the invention. Both alloys had a microstructure of fully lamellar structure as intended, and showed a very long creep rupture time due to sufficient enhancement of gamma-phase strength.

[0099] Alloy 11 is a comparative alloy, and its microstructure is shown in FIG. 17. Alloy 11 represents a comparative alloy with a higher Nb content outside the compositional range according to the invention. A beta phase, seen in white, was observed at a boundary between lamellar colonies. While Nb is a relatively weak beta-phase stabilizing element for TiAl-based alloys, as described hereinbefore, it appears that the addition of excess amount of Nb caused the formation of beta phase. The creep rupture time of Alloy 11 is shorter than the alloys according to the invention

due to inferior high-temperature strength of beta phase.

[00100] Alloys 12-14 are alloys according to the invention, and their respective microstructures are shown in FIGS. 18-20. Alloys 12-14 had different C contents within the compositional range according to the invention. These alloys had a microstructure of lamellar structure, and showed a very long creep rupture time due to sufficient enhancement of gamma-phase strength.

[00101] Alloy 15 is a comparative alloy, and its microstructure is shown in FIG. 21. Alloy 15 represents a comparative alloy with a higher C content outside the compositional range according to the invention. Because of excess C content beyond the solid solubility limit, formation of coarse carbide (Ti_2AlC) was observed. The creep rupture time was therefore shorter than the alloys according to the invention.

[00102] Alloys 16-18 are alloys according to the invention, and their respective microstructures are shown in FIGS. 22-24. Alloys 16-18 had different Si contents within the compositional range according to the invention. These alloys had a microstructure of lamellar structure, and showed a very long creep rupture time due to sufficient strengthening of the entire structure by precipitates and enhancement of gamma-phase strength.

[00103] Alloy 19 is a comparative alloy, and its microstructure is shown in FIG. 25. Alloy 19 represents a comparative alloy with a higher Si content outside the compositional range according to the invention. The creep rupture time was shorter than the alloys according to the invention because a large amount of coarse silicide (Ti_5Si_3) was formed.

[00104] Alloys 20-22 are alloys according to the invention, and their respective microstructures are shown in FIGS. 26-28. Alloys 20, 21 and 23 respectively included addition of 0.75 at.% W, 1.5 at.% Zr, and 1.5 at.% Ta. All of these alloys had a fully lamellar structure similar to those of alloys without such an additional element, and showed further increased creep rupture time by an enhancement of gamma-phase strength by these elements.

[00105] It should be noted that the embodiments and examples described above

are provided merely by way of specific illustration of the present invention, and the present invention should not be construed by way of limitation by the embodiments and examples described above. The TiAl-based alloys of the present invention encompass modifications of the proportion in composition within the scope obvious to those skilled in the art, for example, modifications of the composition within the allowable range necessarily involved in manufacture and/or those within the allowable range according to fluctuations of the purchase price of the base compositions or variance of supply conditions.

[00106] The singular forms "a", "an" and "the" include plural referents unless the context clearly dictates otherwise. Approximating language, as used herein throughout the specification and claims, may be applied to modify any quantitative representation that could permissibly vary without resulting in a change in the basic function to which it is related. Accordingly, a value modified by a term or terms, such as “about” is not limited to the precise value specified. In some instances, the approximating language may correspond to the precision of an instrument for measuring the value. Similarly, “free” may be used in combination with a term, and may include an insubstantial number, or trace amounts, while still being considered free of the modified term.

[00107] The embodiments described herein are examples of articles, systems and methods having elements corresponding to the elements of the invention recited in the claims. This written description enables those of ordinary skill in the art to make and use embodiments having alternative elements that likewise correspond to the elements of the invention recited in the claims. The scope of the invention thus includes articles, systems and methods that do not differ from the literal language of the claims, and further includes other articles, systems and methods with insubstantial differences from the literal language of the claims. While only certain features and embodiments have been illustrated and described herein, many modifications and changes may occur to one of ordinary skill in the relevant art. The appended claims cover all such modifications and changes.

INDUSTRIAL APPLICABILITY

[00108] The TiAl-based alloy as disclosed herein may be suitably used in components operated at higher temperature as compared with those for which conventional TiAl-based alloys have been used. For example, the TiAl-based alloy as disclosed herein may be suitably used as various components in turbomachinery, for example, turbine blades, compressor blades, seals, and other components within industrial gas turbines for power generation; low pressure turbine blades, high pressure compressor blades, shrouds, and seals within aircraft engines for propulsion and auxiliary power generation; impellers, radial compressors, and turbine wheels within turbochargers for diesel and gasoline reciprocating engines.

[00109] The TiAl-based alloy as disclosed herein can be advantageously used for a high-temperature component in power generation gas turbines and/or aviation jet engines with a reduced weight or a larger component size, for which conventional TiAl-based alloys could not be used, whereby contributing to a further reduction of carbon dioxide emission and fuel consumption through improvement of energy efficiency.

LIST OF REFERENCES

1. M. Yamaguchi, et. al.; Recent progress in our understanding of deformation and fracture of two-phase and single-phase TiA1 alloys; ELSEVIER, Materials Science and Engineering A213 (1996) 25-31

2. H.N. Lee, et. al.; Directional solidification and creep deformation of a Ti-46Al-1.5Mo-0.2C (at.%) alloy; ELSEVIER, Intermetallics 10 (2002) 841-850

3. Tetsuya Asai, et. al.; Microstructure in Ti-48at.%Al PST crystal subjected to creep deformation; ELSEVIER, Materials Science and Engineering A329-331 (2002) 828-834

4. K. Maruyama, et. al.; Effects of a 2 spacing on creep deformation characteristics of hard oriented PST crystals of TiAl-based alloy; ELSEVIER, Intermetallics 13 (2005) 1116-1121

5. JP 2008-184665A

6. JP 2000-199025A

7. JP H10-130756A

8. JP H09-176764A

9. JP H07-252562A.

CLAIMS

1. A TiAl-based alloy comprising, in atomic percent (at.%),

about 42.5 % to about 45.5 % aluminum (Al),

about 8.0 % to about 15.0 % niobium (Nb),

about 0.3 % to about 0.8 % carbon (C),

about 0.3 % to about 0.9 % silicon (Si),

balance titanium (Ti) and incidental impurities.

2. The TiAl-based alloy of claim 1, comprising niobium (Nb) in a range from about 9.0 at.% to about 11.0 at.%.

3. The TiAl-based alloy of claim 1, comprising niobium (Nb) in a range from about 9.3 at.% to about 11.0 at.%.

4. The TiAl-based alloy of any of claims 1-3, further comprising at least one element selected from the group consisting of W, Zr, Ta and Cr, in a total amount up to about 3.0 at.%.

5. An article made from the TiAl-based alloy according to any of claims 1-4.

6. The article of claim 5, having a lamellar structure comprising layers of Ti_3Al (alpha2) phase and TiAl (gamma) phase with up to about 20 at.% of primary gamma TiAl.

7. The article of claim 5 or 6, which is substantially free of beta phase.

8. The article of any of claims 5-7, which is turbomachinery components.

9. A turbomachinery comprising the turbomachinery components of claim 8.

10. A turbomachinery of claim 9, which is selected from gas turbines for power generation, aircraft jet engines, industrial gas turbines, and turbochargers for diesel

and gasoline reciprocating engines.

11. A method for producing an article, comprising:

casting a TiAl-based alloy comprising, in atomic percent, about 42.5 % present to about 45.5 % aluminum (Al), about 8.0 % to about 15.0 % niobium (Nb), about 0.3 % to about 0.8 % carbon (C), about 0.3 % to about 0.9 % silicon (Si), balance titanium (Ti) and incidental impurities.

12. A method of claim 11, further comprising:

subjecting the resultant cast to post processing steps.

13. A method of claim 12, wherein the post processing step includes heat treatment at a high temperature, followed by cooling to cause a desired microstructure.

14. A method of claim 12, wherein the post processing step includes forging at a high temperature.

Model material obtained by
directional solidification process
(M. Yamaguchi, et. al.; Materials Science and Engineering A213
(1996) 25-31)

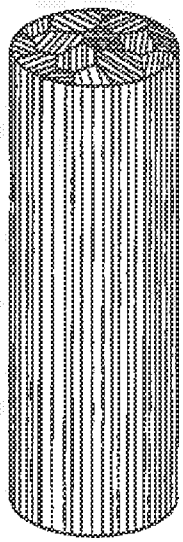

Fig. 2. DS structure composed of columnar grains whose gamma and alpha-2 lamellae are aligned along the growth direction.

FIG. 1

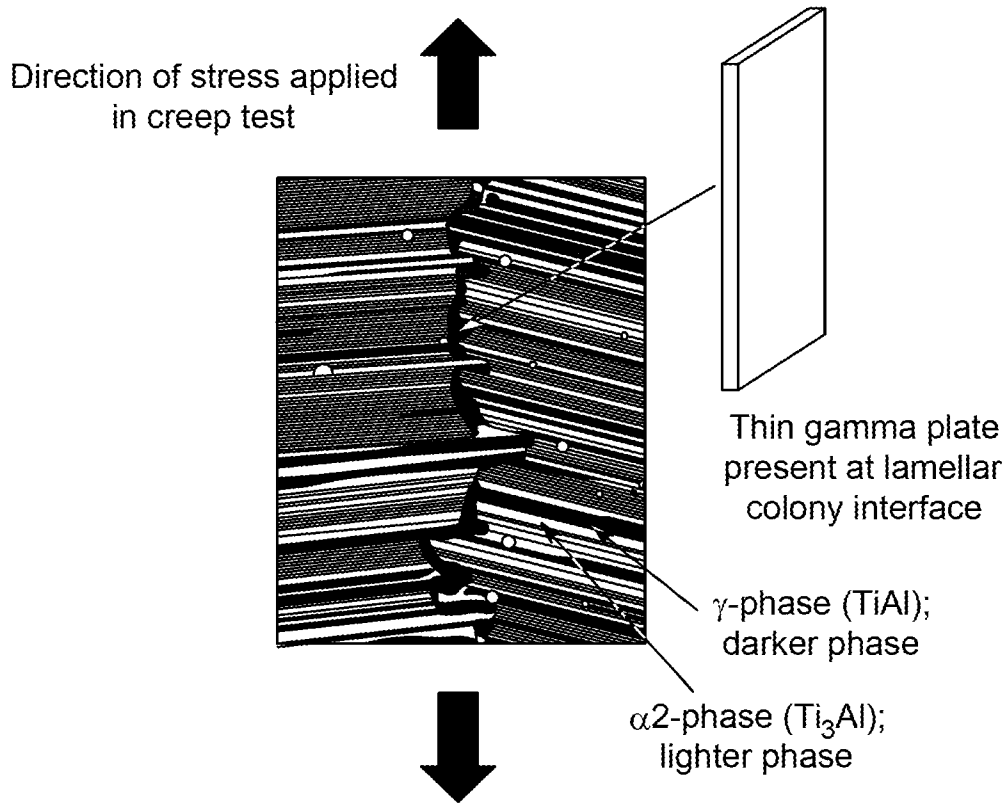

FIG. 2
PRIOR ART

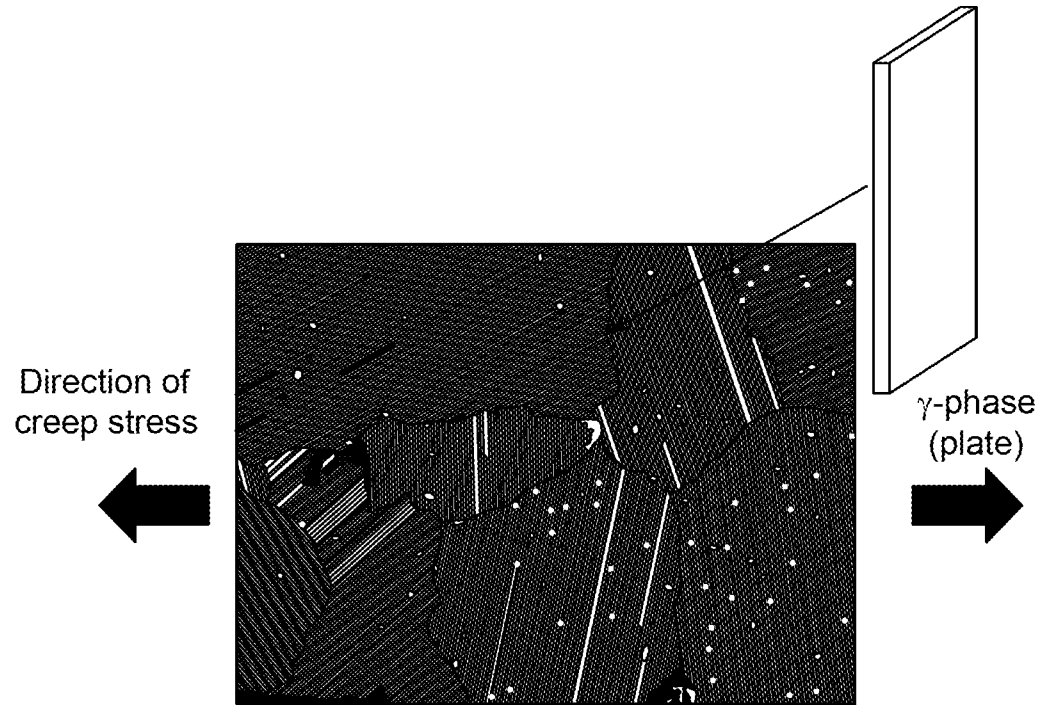
Direction of
creep stress
γ-phase
(plate)

FIG. 3

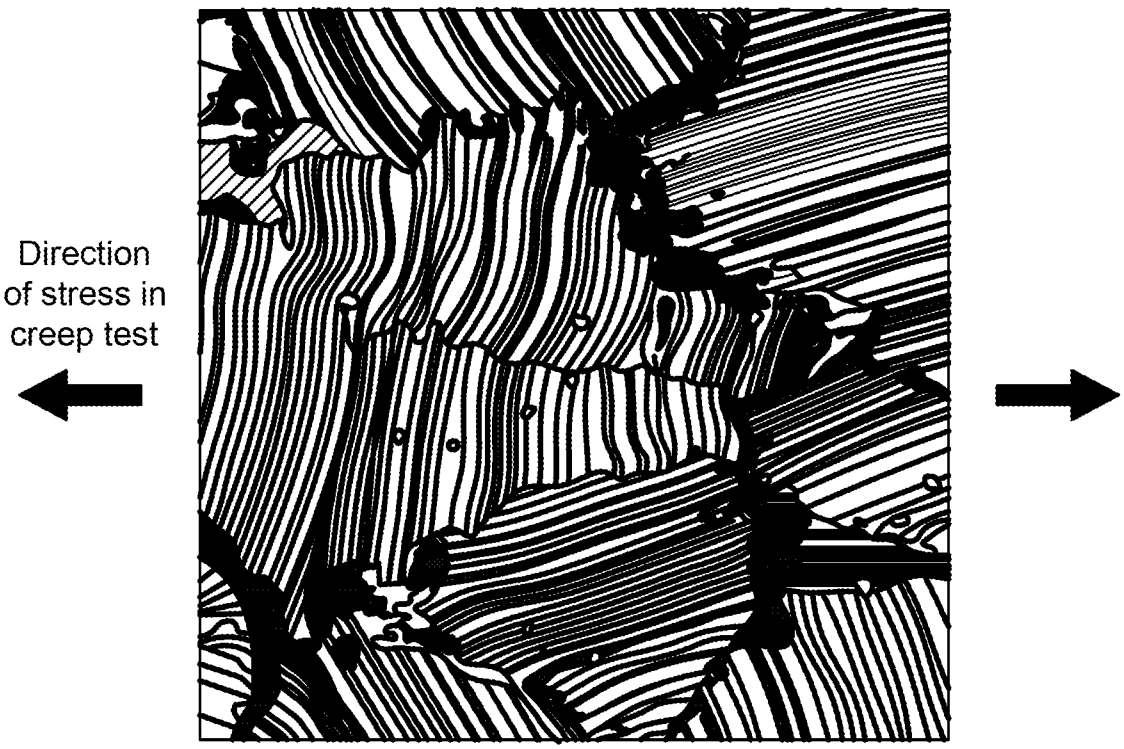
Direction
of stress in
creep test

FIG. 4

Illustrative Microstructure of TiAl-based Alloy having Duplex Structure

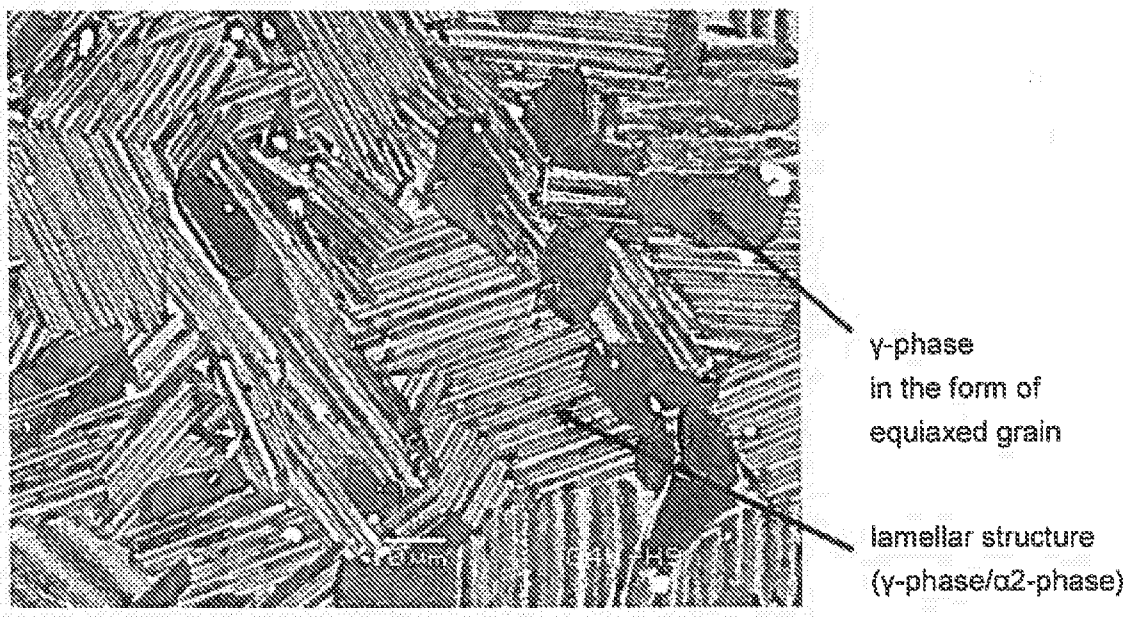

FIG. 5

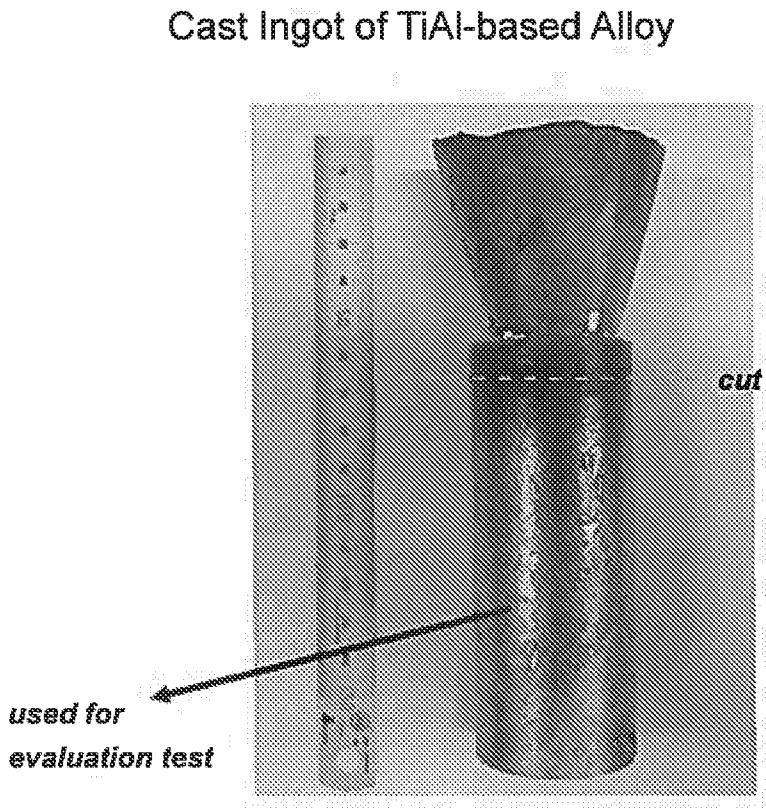

FIG. 6

Microstructure of Alloy 1

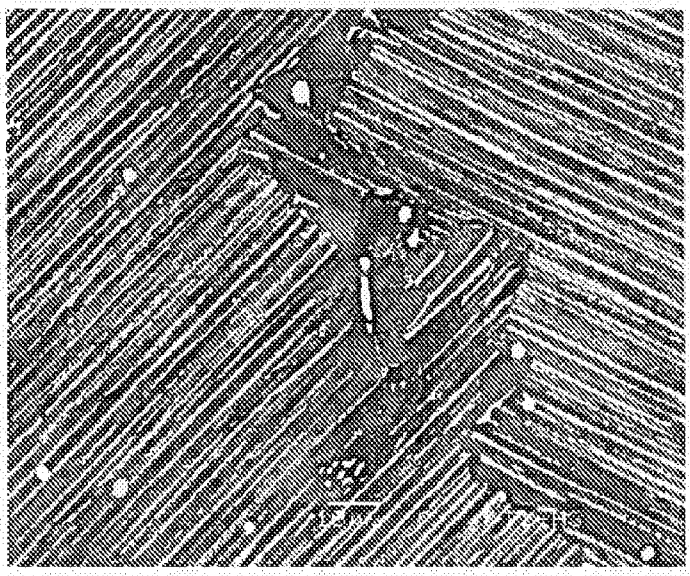

FIG. 7

Microstructure of Alloy 2

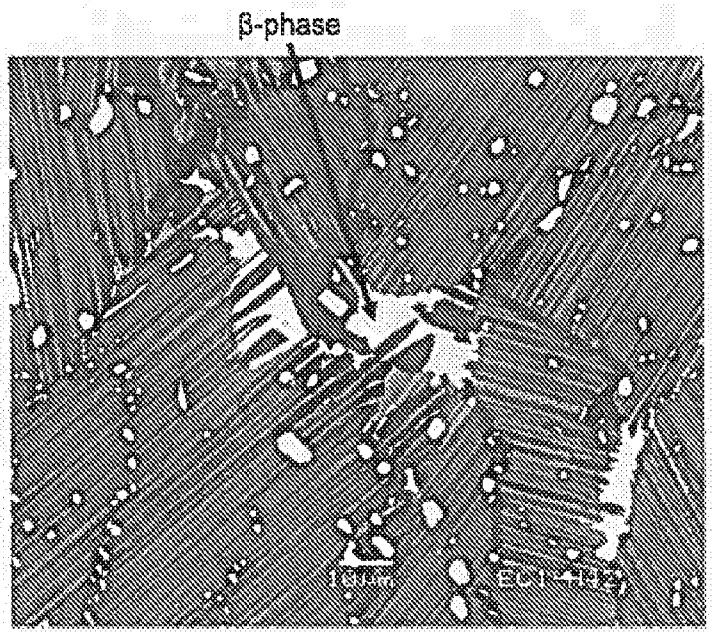

FIG. 8

Microstructure of Alloy 3

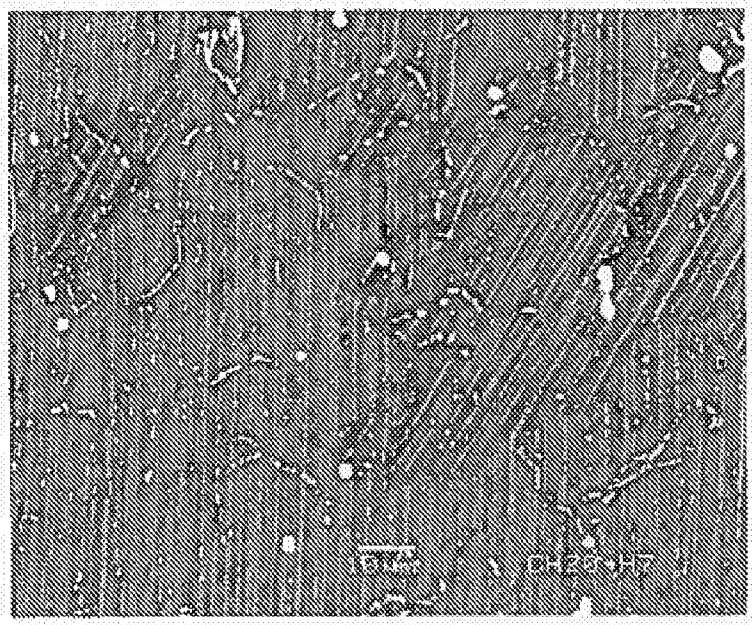

FIG. 9

Microstructure of Alloy 4

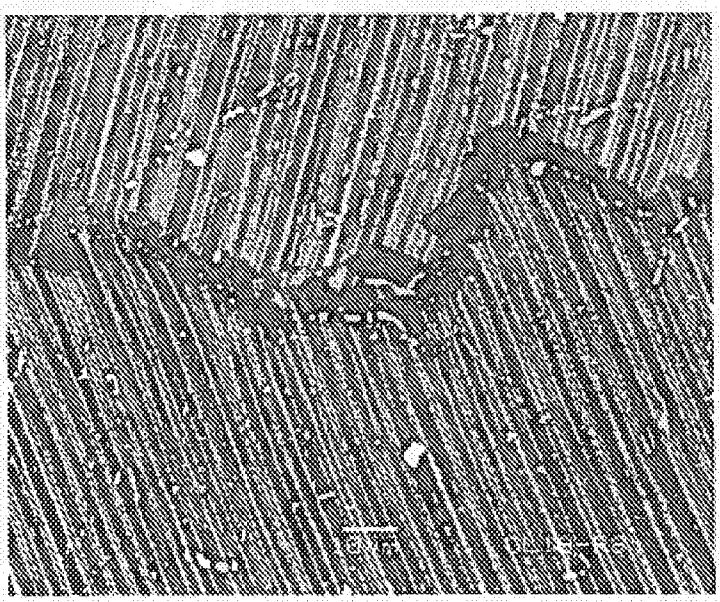

FIG. 10

Microstructure of Alloy 5

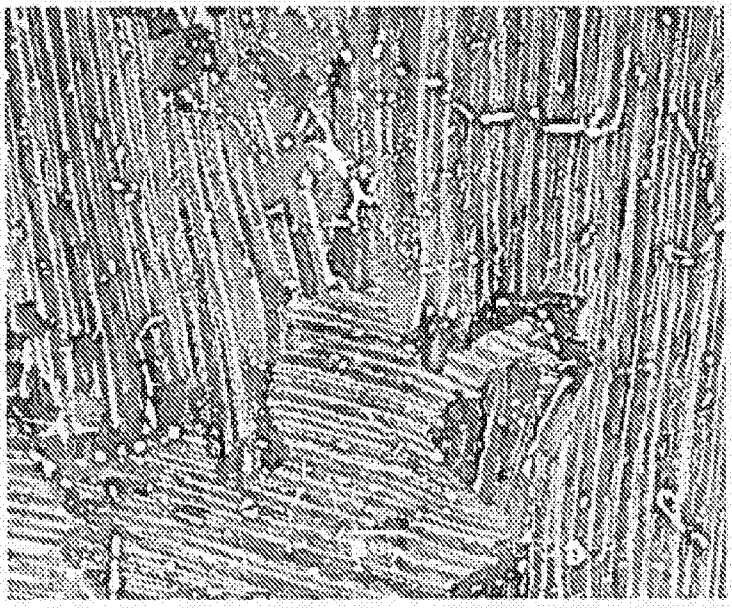

FIG. 11

Microstructure of Alloy 6

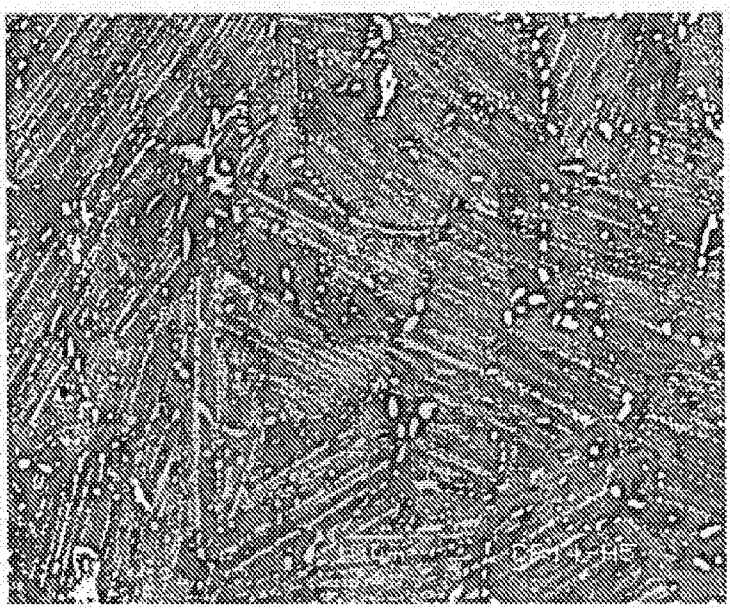

FIG. 12

Microstructure of Alloy 7

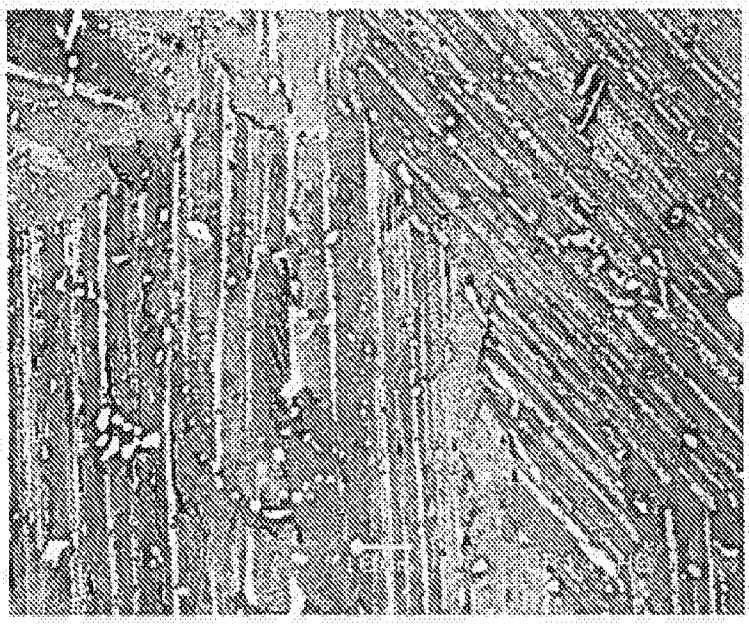

FIG. 13

Microstructure of Alloy 8

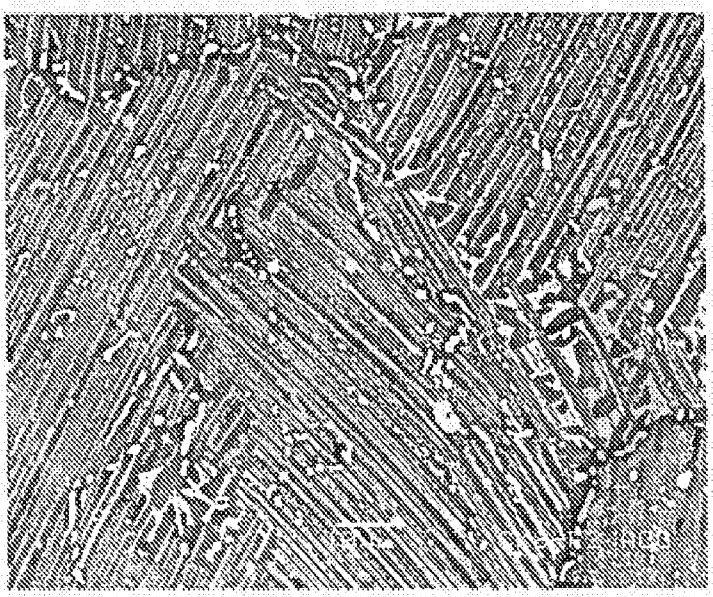

FIG. 14

Microstructure of Alloy 9

FIG. 15

Microstructure of Alloy 10

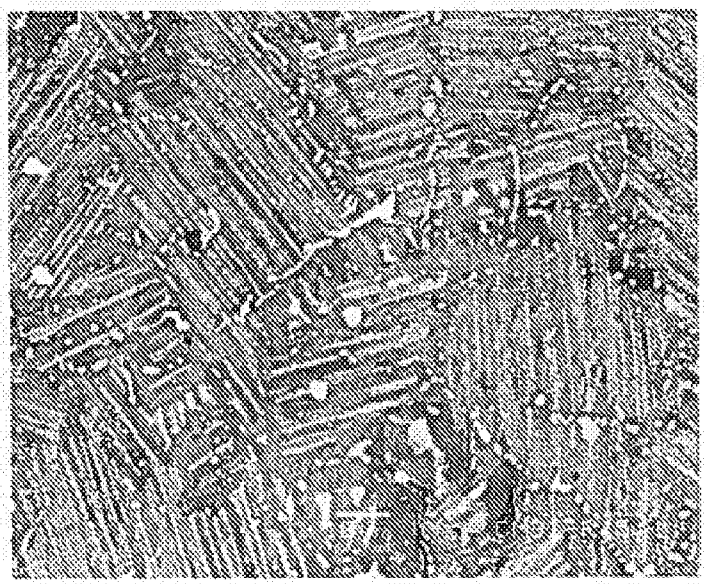

FIG. 16

Microstructure of Alloy 11

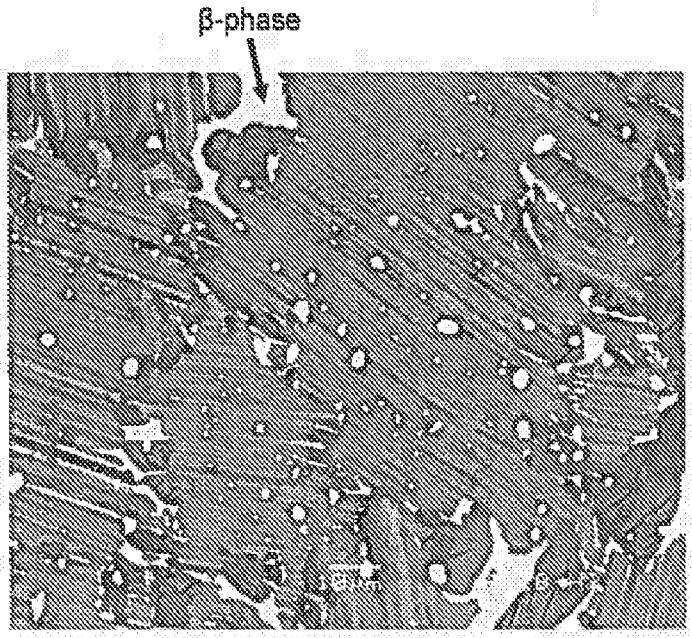

FIG. 17

Microstructure of Alloy 12

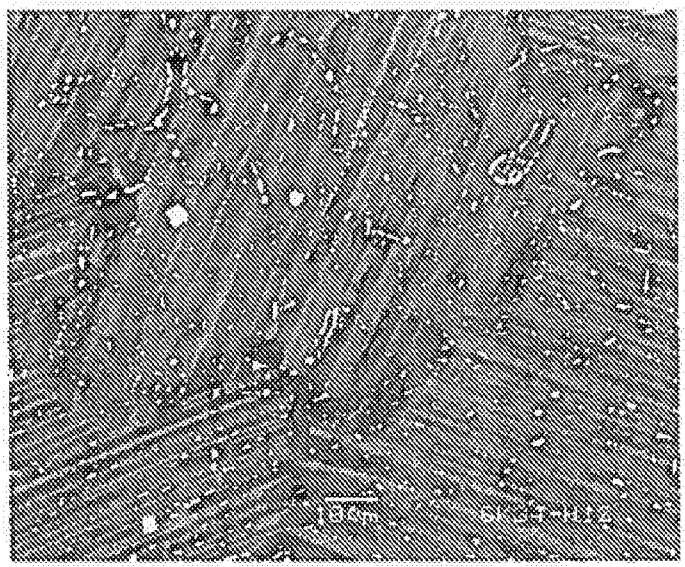

FIG. 18

Microstructure of Alloy 13

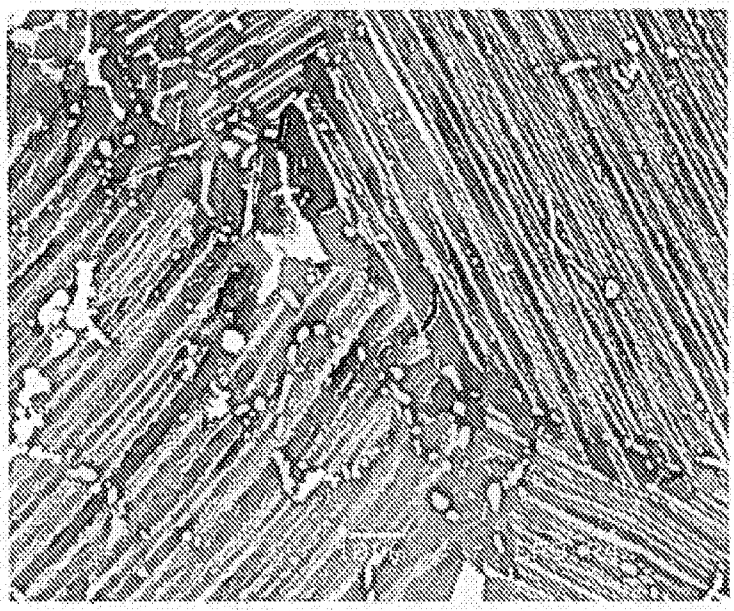

FIG. 19

Microstructure of Alloy 14

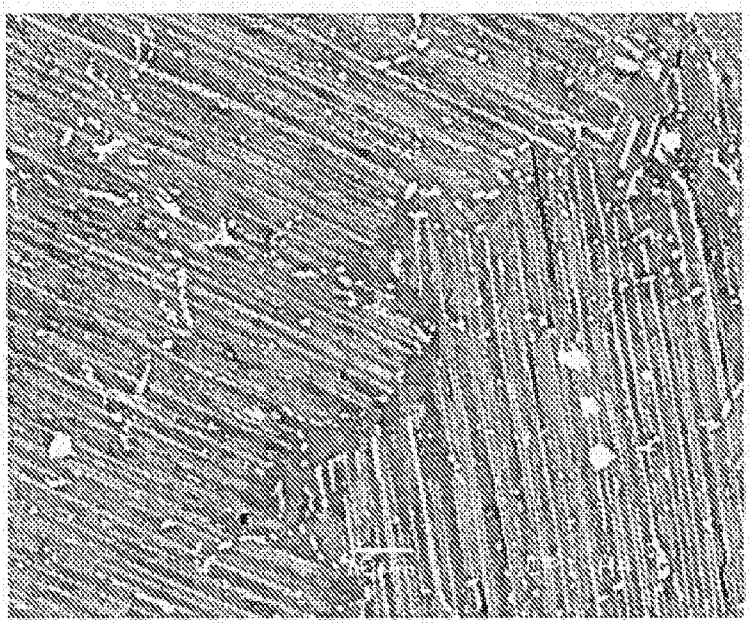

FIG. 20

Microstructure of Alloy 15

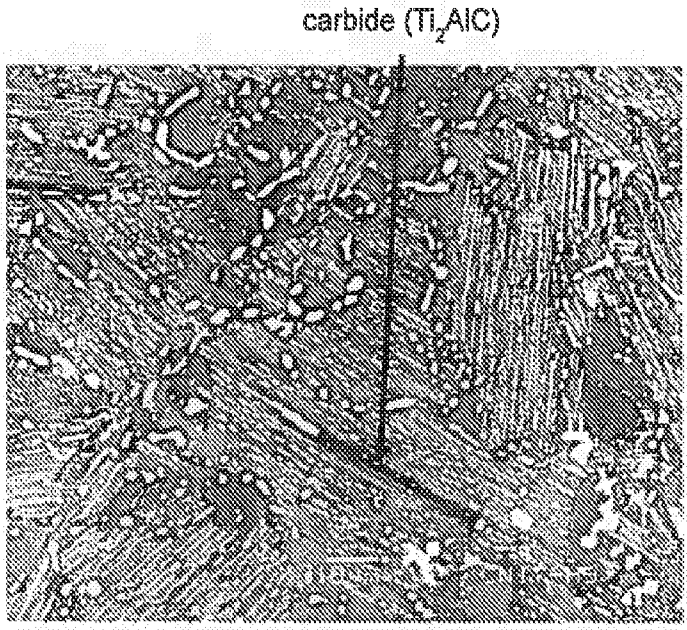

FIG. 21

Microstructure of Alloy 16

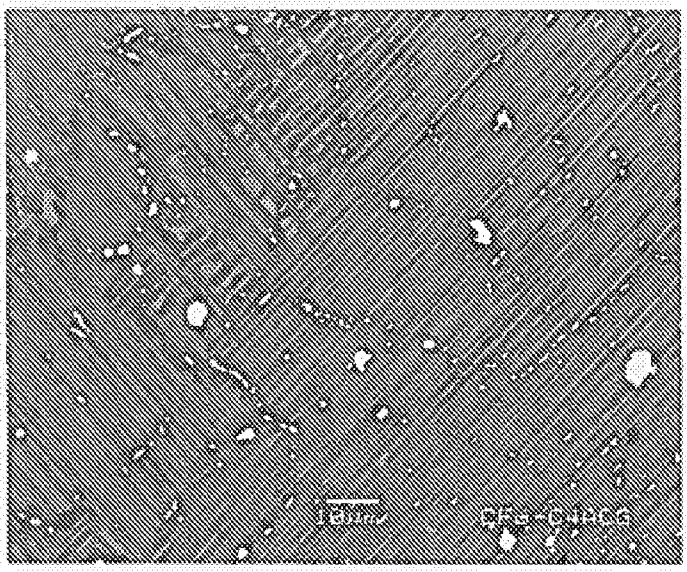

FIG. 22

Microstructure of Alloy 17

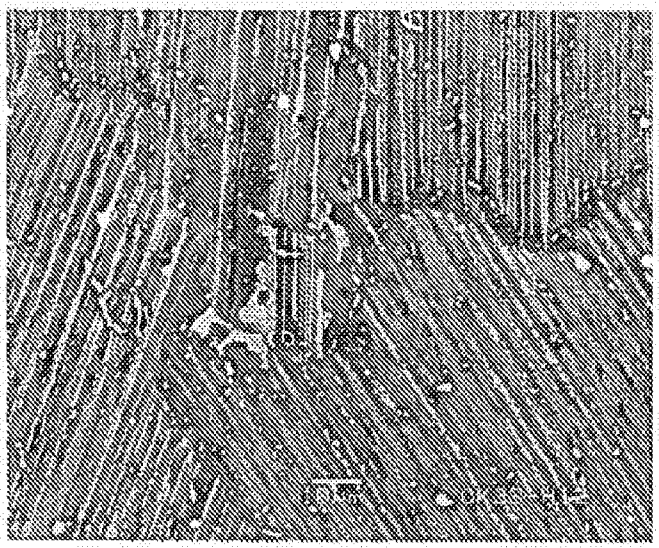

FIG. 23

Microstructure of Alloy 18

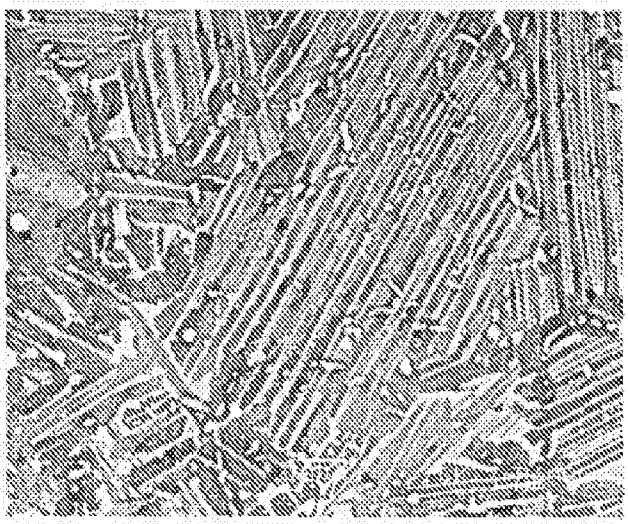

FIG. 24

Microstructure of Alloy 19

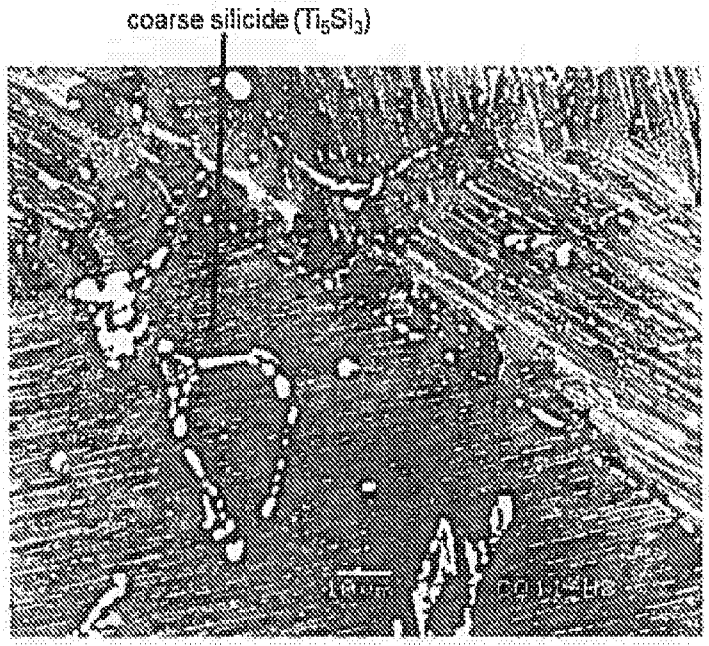

FIG. 25

Microstructure of Alloy 20

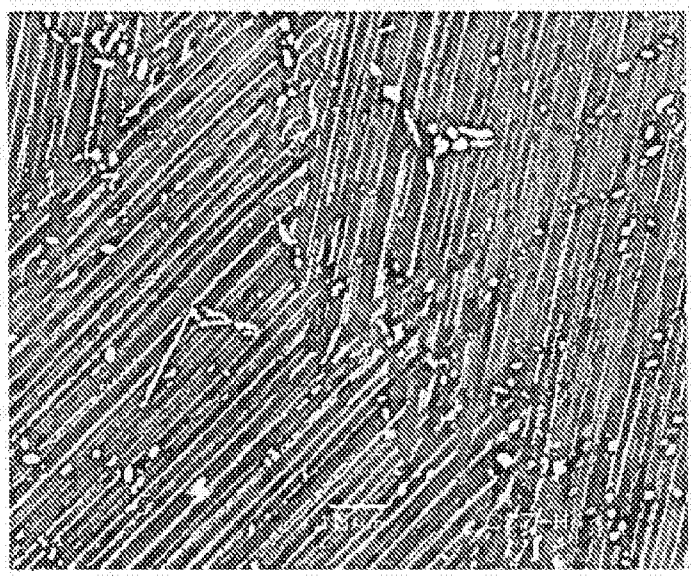

FIG. 26

Microstructure of Alloy 21

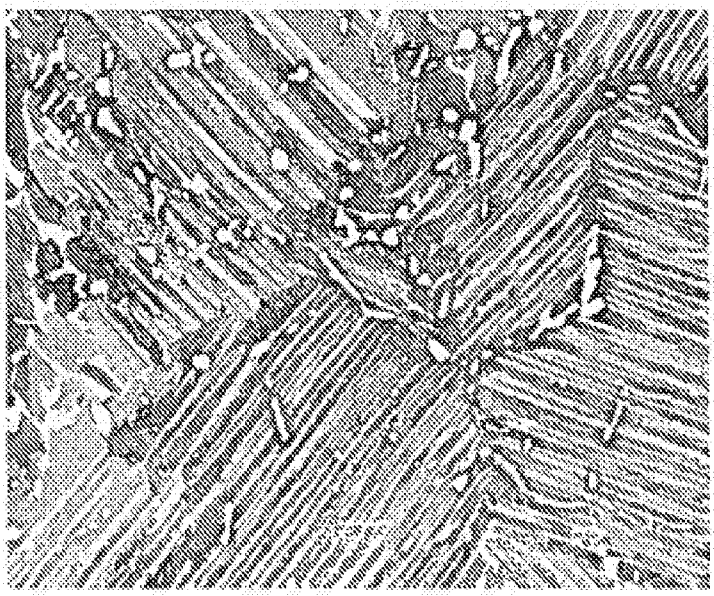

FIG. 27

Microstructure of Alloy 22

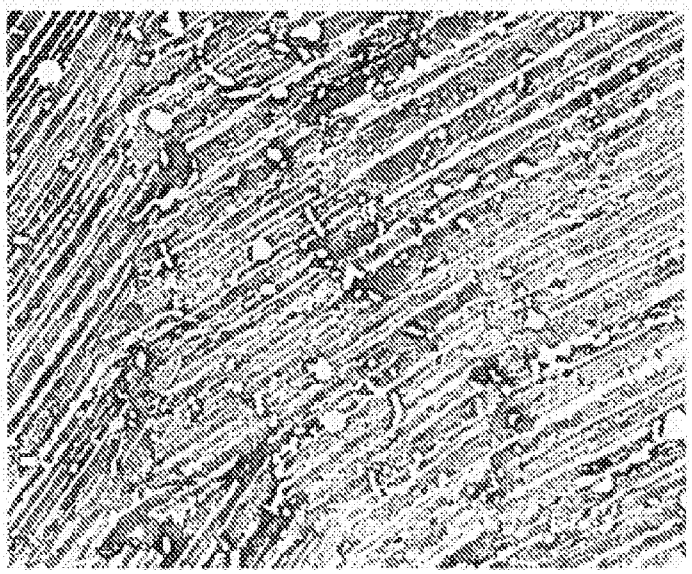

FIG. 28

INTERNATIONAL SEARCH REPORT

International application No
PCT/US2016/012786

A. CLASSIFICATION OF SUBJECT MATTER
INV. C22C14/00 C22F1/18
ADD.

According to International Patent Classification (IPC) or to both national classification and IPC

B. FIELDS SEARCHED

Minimum documentation searched (classification system followed by classification symbols)
C22C C22F

Documentation searched other than minimum documentation to the extent that such documents are included in the fields searched

Electronic data base consulted during the international search (name of data base and, where practicable, search terms used)
EPO-Internal, WPI Data

C. DOCUMENTS CONSIDERED TO BE RELEVANT

Category*	Citation of document, with indication, where appropriate, of the relevant passages	Relevant to claim No.
X	WO 2015/182454 A1 (NAT INST FOR MATERIALS SCIENCE [JP]) 3 December 2015 (2015-12-03) paragraphs [0001], [0008], [0009], [0010]; table 1	1-14
E	EP 3 012 337 A1 (NAT INST FOR MATERIALS SCIENCE [JP]) 27 April 2016 (2016-04-27) paragraphs [0001], [0003], [0004], [0011], [0012], [0017], [0018], [0047], [0071]	1-14

☐ Further documents are listed in the continuation of Box C.

☒ See patent family annex.

* Special categories of cited documents :

"A" document defining the general state of the art which is not considered to be of particular relevance

"E" earlier application or patent but published on or after the international filing date

"L" document which may throw doubts on priority claim(s) or which is cited to establish the publication date of another citation or other special reason (as specified)

"O" document referring to an oral disclosure, use, exhibition or other means

"P" document published prior to the international filing date but later than the priority date claimed

"T" later document published after the international filing date or priority date and not in conflict with the application but cited to understand the principle or theory underlying the invention

"X" document of particular relevance; the claimed invention cannot be considered novel or cannot be considered to involve an inventive step when the document is taken alone

"Y" document of particular relevance; the claimed invention cannot be considered to involve an inventive step when the document is combined with one or more other such documents, such combination being obvious to a person skilled in the art

"&" document member of the same patent family

Date of the actual completion of the international search	Date of mailing of the international search report
25 August 2016	02/09/2016

Name and mailing address of the ISA/	Authorized officer
European Patent Office, P.B. 5818 Patentlaan 2 NL - 2280 HV Rijswijk Tel. (+31-70) 340-2040, Fax: (+31-70) 340-3016	Brown, Andrew

1

INTERNATIONAL SEARCH REPORT

Information on patent family members

International application No
PCT/US2016/012786

Patent document cited in search report	Publication date	Patent family member(s)	Publication date
WO 2015182454 A1	03-12-2015	JP 2015224372 A	14-12-2015
		WO 2015182454 A1	03-12-2015
EP 3012337 A1	27-04-2016	EP 3012337 A1	27-04-2016
		US 2016145703 A1	26-05-2016
		WO 2014203714 A1	24-12-2014